Macromolecules

ARTICLE

pubs.acs.org/Macromolecules

# L-Proline Functionalized Polymers Prepared by RAFT Polymerization and Their Assemblies as Supported Organocatalysts

Annhelen Lu,[†] Thomas P. Smart,[‡] Thomas H. Epps, III,[‡] Deborah A. Longbottom,[*,§] and Rachel K. O'Reilly[*,†]

[†]Department of Chemistry, University of Warwick, Gibbet Hill Road, Coventry, CV4 7AL, United Kingdom

[‡]Department of Chemical Engineering, University of Delaware, 150 Academy Street, Newark, Delaware 19716, United States

[§]Department of Chemistry, University of Cambridge, Lensfield Road, Cambridge, CB2 1EW, United Kingdom

Supporting Information

**ABSTRACT:** We have prepared a range of well-defined copolymers of styrene and L-proline functionalized styrene (5−11 kDa) using reversible addition−fragmentation chain transfer (RAFT) polymerization techniques and explored their use in supported catalysis. Upon deprotection of the L-proline functionalities, the solution self-assembly of these copolymers was investigated in mixed solvent systems. The resulting assemblies were characterized by dynamic light scattering, transmission electron microscopy (on graphene oxide substrates, along with cryo-TEM and tomography), and scanning electron microscopy. The application of these functional assemblies as supported catalysts for the aldol condensation reaction was explored using cyclohexanone and 4-nitrobenzaldehyde. The rate and selectivity of solution catalysis in our self-assembled system were comparable to those of L-proline, and a significant advantage of our system was that the polymer support could be utilized at lower catalyst loadings with comparable activity and also could be recycled a number of times while maintaining activity and selectivity.

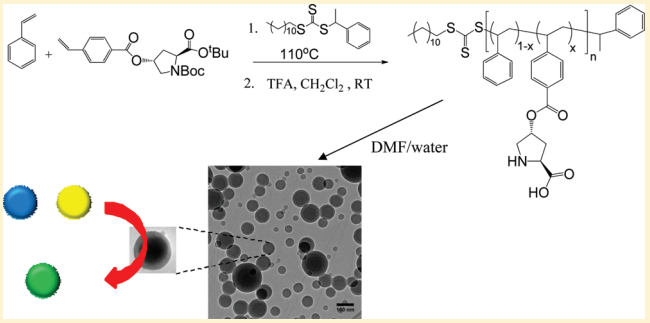


## INTRODUCTION

The use of organic molecules as catalysts in asymmetric reactions has garnered great attention in recent years as these molecules serve as attractive alternatives to transition metal and enzyme based catalysts.[1−3] This class of catalysts, named organocatalysts, are not only often less expensive but also sometimes readily available from the chiral pool and experimentally tractable, as the majority of them are stable to both water and oxygen.[1,4,5]

Nature's aldolase enzymes carry out the asymmetric aldol reaction via an enamine based mechanism,[6−8] and the amino acid L-proline has been named the "simple enzyme", as it is proposed to mimic the aldolase enzymes in this mechanistic aspect.[9] The organocatalytic properties of L-proline were first reported in the 1970s by Hajos and Parrish[10] and Eder et al.,[5] and L-proline has since become one of the most popular organocatalysts in asymmetric synthesis. L-Proline and its derivatives (Figure 1) are highly effective and selective catalysts used in a number of asymmetric reactions including Mannich reactions,[4,11] Michael additions,[12,13] Robinson annulations,[14] and aldol condensation reactions.[4,6] These reactions are of interest as a new asymmetric carbon−carbon bond is formed, and thus they are often key steps in the synthesis of natural products and non-natural drug molecules.[8,15]

Thus, much research has been concentrated on improving the performance of L-proline via modifications to the active centers and in particular the acid functionality. Barbas,[16,17] Hayashi,[18] and others[19,20] showed high selectivity with some of their derivatives; however, a number of derivatives have also resulted in reduced performance.[21−23] These studies highlight the key role of sterics and electronics around the active centers of the L-proline in mediating highly selective and efficient catalysis. Additionally, it has been suggested that the presence of a polymer scaffold may have a beneficial influence on the catalyst activity, as it can to an extent be considered as a peptide-backbone mimic. Therefore, great efforts have been dedicated to the immobilization of L-proline on solid supports to enhance catalytic activity as well as to facilitate the recycle and reuse of the catalyst.[24]

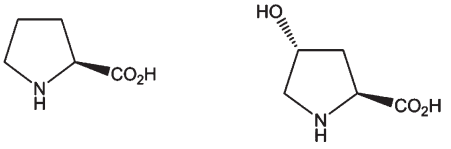


**Figure 1.** Structures of the bifunctional organocatalysts L-proline (left) and its derivative 4-hydroxy-L-proline (right).

**Received:** June 3, 2011
**Revised:** August 13, 2011
**Published:** September 06, 2011

**Scheme 1. Coupling Reaction of 1 and VBA To Give Monomer 2**

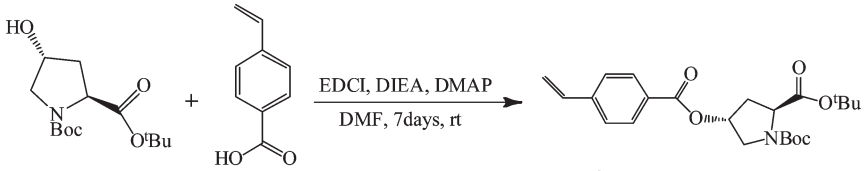


Benaglia and co-workers[25−27] have anchored L-proline onto a poly(ethylene glycol) (PEG) scaffold, which was successfully recovered and reused several times in the aldol condensation, with close to unchanged yields and only small losses in selectivity. Polystyrene (beads),[28−31] Merrifield resin,[32] ionic liquids,[33,34] and dendrimers[35] are examples of other reported supports for L-proline. While these studies highlight the potential to selectively incorporate L-proline into a polymer scaffold without a loss in activity, the selective incorporation of L-proline functionalized monomers into polymers is a less well-explored area. This is somewhat surprising given the pioneering work of Endo and Sanda[36] and more recently others on the preparation, polymerization, and properties of a range of vinyl amino acid monomers including L-phenylalanine, L-leucine, L-alanine, and L-histidine.[37−40]

In recent years the group of Hansen and co-workers[24,41,42] has reported the synthesis of several L-proline functionalized methacrylate monomers and a range of L-proline functionalized styrenic and methacrylic copolymer beads. The L-proline functionalized beads showed both high activity and selectivity in water and were successfully recycled five times without a significant loss in catalytic activity. Although this technique may be used on a large industrial scale, with simple work-up and purification and good control of catalyst loading, this type of (co)polymerization technique does not allow for the controlled synthesis of more complex or well-defined polymer architectures such as block copolymers/amphiphiles, which may undergo self-assembly to form higher-order structures and perhaps find utility as organocatalytic nanoreactors.[43]

To obtain improved copolymerization polydispersity control, controlled radical polymerization (CRP) techniques are often employed instead of conventional free radical methods. In particular, the application of reversible addition−fragmentation chain transfer (RAFT) polymerization for the preparation of well-defined functional copolymers has received much attention in the past decade.[44−53] RAFT polymerization is a versatile polymerization technique as it proceeds under relatively mild reaction conditions, is highly tolerant to a variety of monomers including monomers with unprotected functional groups (such as acids, alcohols, and amines), and is amenable to a number of postpolymerization modifications including end-group removal and chain extension to afford well-defined block copolymers.

Indeed, Endo and co-workers[54−57] have reported the successful use of RAFT techniques to incorporate L-proline and 4-hydroxy-L-proline units into a polyacrylamide backbone, though not leaving the key amine functionality available to play its essential role in the aldol reaction. More recently, our group has reported the successful synthesis of L-proline functionalized polystyrene copolymers[58,59] via both nitroxide-mediated polymerization (NMP)[58] and RAFT polymerization techniques.[59] The organocatalytic activity and selectivity of the copolymers synthesized via the NMP technique were carefully studied in a typical aldol reaction. Various solvents were screened, and the mixed solvent systems with DMSO/water and DMF/water gave the most promising results. Conversions of up to 95%, anti/syn ratios up to 95/5, and enantiomeric excesses up to 94% were achieved when the aldol reaction was carried out in the mixed solvent systems. These findings were not entirely unexpected, as water has been reported to enhance the rate of reaction, as it helps promote the formation of the enamine transition state.[60−64] Given these initial promising results, we are further exploring this chemistry with our RAFT derived polymers to allow for access to highly active recyclable supports. Furthermore, we propose that the selective incorporation of the hydrophilic amino acid L-proline into a hydrophobic polystyrene backbone will yield polymers with tunable solution properties to allow for self-assembly of the resultant copolymers. We hypothesize that the formation of higher order assemblies will affect the catalytic activity of the L-proline in the copolymers and allow for improved postreaction catalyst recovery. These self-assembly effects on activity and recovery are explored in this work.

## RESULTS AND DISCUSSION

**Monomer Synthesis.** To afford the means to attach the organocatalytically active L-proline to the polymer backbone, while leaving both the amino and carboxylic acid functionalities of the L-proline available for catalysis, a bis-protected 4-hydroxy-L-proline functionalized monomer, protected at the amino and acid functionalities, was synthesized. First, commercially available Boc-*O*-benzyl-L-hydroxyproline was modified via two protection/deprotection reactions to yield **1**.[65] Then, precursor **1** was coupled with 4-vinylbenzoic acid (VBA) via the Steglich esterification[66] reaction to provide the desired bis-protected L-proline functionalized styrenic monomer **2** (Scheme 1). Our group has previously shown that this coupling technique does not result in the racemization of the key chiral C2 carbon.[59]

The amino and acid functionalities on L-proline were protected with a *tert*-butyloxycarbonyl (Boc) group and a *tert*-butyl ester ($^t$Bu) group, respectively. These protecting groups were selected due to the simple deprotection strategy that may be employed to simultaneously reveal both the L-proline carboxylic acid and amino functionalities.[67] This deprotection strategy was more straightforward than the benzyl carbamate (Cbz) and benzyl ester (Bn) protection methodology previously reported by our group.[59] The resultant monomer **2** was characterized by $^1$H and $^{13}$C NMR spectroscopy, high-resolution mass spectroscopy (HR-MS), IR, and elemental analysis; the IR spectrum is shown in Figure S1. A number of signals in the $^1$H NMR spectrum of **2** showed unexpected splitting patterns, and thus the assignment of the protons present in the L-proline five-membered ring (labeled f−i in Figure 2) was initially explored using 2D COSY NMR spectroscopy. The observed splitting patterns of the protons labeled g and i arise because these protons

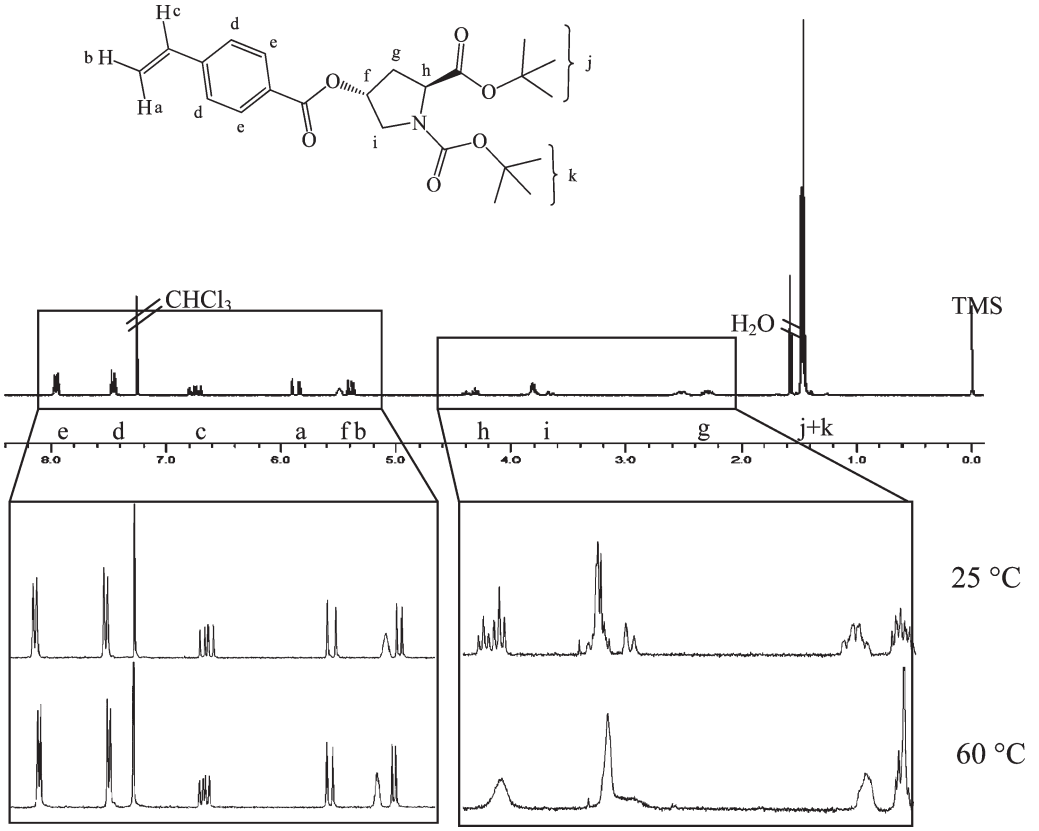


**Figure 2.** $^1$H NMR (400 MHz) spectrum of monomer **2**, in $CDCl_3$ at 25 °C and 60 °C.

**Scheme 2. Scheme Representing Bulk Copolymerization of 2 with Styrene Using 3 as CTA To Give Copolymers 4**

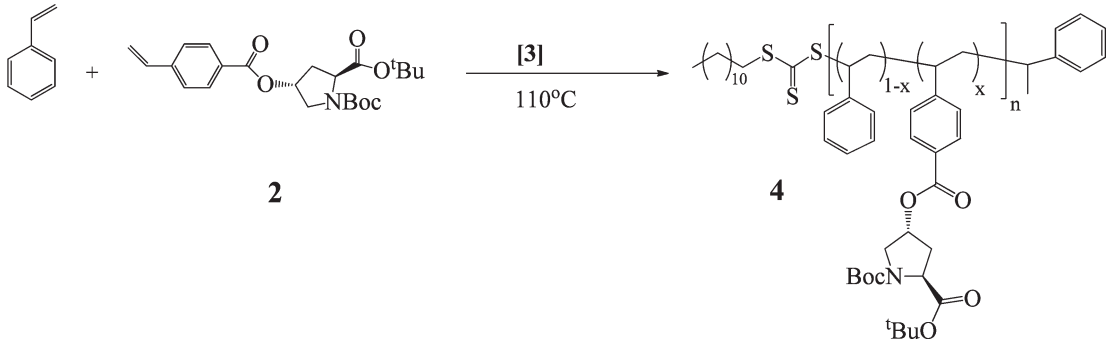


are situated between two stereocenters in the ring and experience different environments, causing the splitting pattern shown in Figure 2. The unusual splitting noted at $\delta$ 4.30 (proton h) was due to a rotameric effect of the neighboring Boc N-protecting group, which was resolved by high-temperature $^1$H NMR spectroscopy at 60 °C in $CDCl_3$, verifying that no racemization had taken place during the coupling process.

**Copolymerization of Functionalized Monomer with Styrene Using RAFT.** RAFT polymerization was utilized to incorporate the L-proline functionalized monomer into a polystyrene based copolymer (Scheme 2). Dodecyl 1-phenylethyl trithiocarbonate **3** (Figure S2) was used as the RAFT agent, or chain transfer agent (CTA), as trithiocarbonates are suitable for the polymerization of styrene and styrenic monomers.[68−70]

The polymerization resulted in the desired catalyst loading on the polymer (ca. 5%), with a narrow polydispersity index (ca. 1.1), showing the polymerization proceeded with good control. Percentage conversion of the two monomers was determined by comparing distinct monomer signals ($\delta$ 5.30 ppm for L-proline and $\delta$ 5.13 ppm for styrene) to a distinct polymer signal at $\delta$ 5.45 ppm for L-proline and $\delta$ 6.20−7.30 ppm for polystyrene (Figure S3), and the $^1$H NMR signals were utilized to estimate the molecular weight of the resultant copolymer. Percentage incorporation of **2** was determined by comparing a polymer signal in the $^1$H NMR spectrum for each monomer to a distinct end-group signal from the chain transfer agent, CTA (at $\delta$ 3.20 ppm). This information was further used to confirm the molecular weight of the copolymer; however, it should be noted this method assumes

**Table 1. Copolymerization Data for 2 and Styrene, with 95:5:1 Ratio of Styrene:2:3, Polymerization in Bulk at 110 °C (Reaction Quenched Depending on the Desired DP of Styrene)**

| polymer | DP[a] | DP[b] | $M_n$[c] (kDa) | $M_n$[d] (kDa) | $M_w/M_n$[d] | % incorporation of 2[c] |
|---|---|---|---|---|---|---|
| **4a** | 93 | 4 | 11.7 | 9.5 | 1.06 | 4.0 |
| **4b** | 34 | 3 | 5.2 | 5.0 | 1.07 | 8.0 |
| **4c** | 65 | 3 | 8.4 | 8.7 | 1.06 | 4.5 |
| **4d** | 64 | 3 | 8.3 | 8.5 | 1.13 | 4.5 |
| **4e** | 93 | 3 | 11.6 | 9.5 | 1.07 | 3.0 |
| **4f** | 83 | 4 | 10.3 | 12.3 | 1.07 | 4.6 |
| **4g** | 74 | 4 | 10.2 | 11.6 | 1.07 | 5.0 |

[a] Of styrene, determined by $^1$H NMR spectroscopy, in $CDCl_3$. [b] Of **2**, determined by $^1$H NMR spectroscopy, in $CDCl_3$. [c] Determined by $^1$H NMR spectroscopy, in $CDCl_3$. [d] Determined by GPC, in THF, PS calibration.

100% end-group fidelity. The presence of the CTA end group in the copolymers was confirmed by examining the UV trace signal collected from GPC analysis at 309 nm, the wavelength characteristic for the trithiocarbonate end group.

Additionally, the active functionalities of monomer **2** were deprotected prior to polymerization (see Supporting Information), and this new monomer could be successfully copolymerized using RAFT with styrene (under the same conditions highlighted in Table 1) to afford a copolymer of similar composition to the protected analogue ($M_{n,NMR}$ = 14.3 kDa, Figure S5); however, its SEC characterization was difficult due to the amphiphilic nature of the copolymers, and hence the protected monomer **2** was used in this study.

**Reactivity Ratio of Copolymerization.** Previous initial investigations into the copolymerization kinetics carried out in our group suggested a faster polymerization rate for monomer **2** compared to styrene.[59] This led us to hypothesize a nonrandom polymerization and instead propose a gradient-type structure for these L-proline−styrene copolymers **4**. To confirm this hypothesis, the reactivity ratios of the two monomers in this copolymerization were investigated; thus, different ratios of the two monomers (styrene/**2** with ratios 90/10, 80/20, 70/30, 60/40, and 50:50) were polymerized with **3** under the same conditions (in bulk at 110 °C). An aliquot was taken after 30 min to determine the conversion by $^1$H NMR spectroscopy. The mole ratio of each monomer in the resultant copolymer and the initial monomer feed were used to determine the reactivity ratios of the monomers. The linearized Finemann−Ross (FR) model was used for this analysis,[71] and the model concluded that $r_1 > r_2$ ($r_1$ = 9.3; $r_2$ = 0.11), in the case where monomer **2** is $M_1$ and styrene is $M_2$, suggesting blocklike polymerization and thus validating our hypothesis as to the nature of the copolymer. The parameters used to calculate $r_1$ and $r_2$ using the FR model are given in Table S1.

Additionally, Contour, a computer program developed by van Herk[72] using a nonlinear least-squares fitting method, was used to investigate our copolymer system. The $F_1$ and $f_1$ values of the copolymerization were entered into the program, and a set of calculations were performed to rapidly determine the reactivity ratio of the two monomers that fits the input criterion, where $F_1$ = copolymer composition and $f_1$ = feed composition. The generated values for $r_1$ and $r_2$ were 12.4 and 0.01, respectively, and

**Table 2. Data Showing Conversion, Final Diastereomeric Ratio (dr), and Enantiomeric Excess (ee), Using Copolymer 5c at 20 mol % and Unsupported L-Proline at 20 mol % after 24 h**

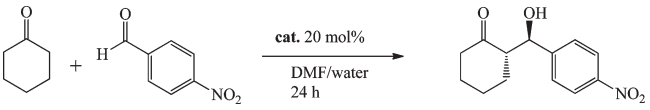


| entry | cat. | % water in DMF | % conv HPLC | % conv NMR | anti/syn[a] | % ee[b] |
|---|---|---|---|---|---|---|
| 1 | **5c** | 0 | 50 | 49 | 89/11 | 91 |
| 2 | **5c** | 5 | 90 | 98 | 95/5 | 89 |
| 3 | **5c** | 7.5 | 82 | 90 | 95/5 | 85 |
| 4 | **5c** | 12 | 87 | 90 | 91/9 | 94 |
| 5 | L-proline | 0 | | 21 | 91/9 | 83 |
| 6 | L-proline | 5 | 99 | 99 | 92/9 | 86 |
| 7 | L-proline | 7.5 | 99 | 99 | 92/8 | 88 |
| 8 | L-proline | 12 | 97 | 98 | 87/13 | 82 |

[a] Determined by $^1$H NMR spectroscopy in $CDCl_3$. [b] Determined by chiral HPLC, Chiralpak IA column (80:20 hexane:IPA).

$r_1 \times r_2 \sim 1$, confirming an extreme ideal copolymerization given the very different reactivity ratios for the pair of monomers. This difference in reactivity ratios implies that $M_1$ (monomer **2**) is preferentially added to the propagating species, supporting results obtained via the linear model. A plot showing this extreme ideal behavior generated in Contour is shown in Figure S5. This behavior is not entirely unexpected as the presence of the electron-withdrawing ester linkage present at the para-position on monomer **2** is expected to increase the rate of polymerization of **2** compared to that of styrene. However, we propose that this nonrandom distribution of monomer **2** in the polymer backbone will lead to an amphiphilic copolymer (once monomer **2** is deprotected), potentially allowing for interesting self-assembly behavior.[73,74]

**Polymer Deprotection.** The Boc and $^t$Bu protecting groups for the amine and carboxylic acid, respectively, can be readily deprotected under acidic conditions.[67] Thus, copolymers **4a**−**g** were deprotected in dry $CH_2Cl_2$ in the presence of trifluoroacetic acid (TFA) to afford copolymers **5a**−**g**. Successful deprotection was confirmed by comparing signals the $^1$H NMR data given in Figures S3 and S4. The $^t$Bu signals disappeared following deprotection, causing a simplification in the 1.15−2.60 ppm region, and the characteristic L-proline signal from the proton labeled "a" has now shifted from $\delta$ 5.45 to 5.63 ppm (Figure S4). To confirm that the ester, which links the catalytically active L-proline moiety to the polymer backbone, was not also affected under these strong acidic conditions, monomer **2** was stirred in TFA under the deprotection conditions. Under these conditions the L-proline was successfully deprotected, and the ester linkage was found to be stable.

**Organocatalytic Properties of L-Proline Functionalized Polymer.** The catalytic activity of the synthesized L-proline functionalized copolymers (**5a**−**g**) was tested using a representative aldol reaction between cyclohexanone and 4-nitrobenzaldehyde. This system has been previously studied with other solid-supported L-proline catalysts, and thus the catalyst activity can be directly compared.[29,32,75] Previously, our group has shown that our NMP copolymers with different catalyst incorporations

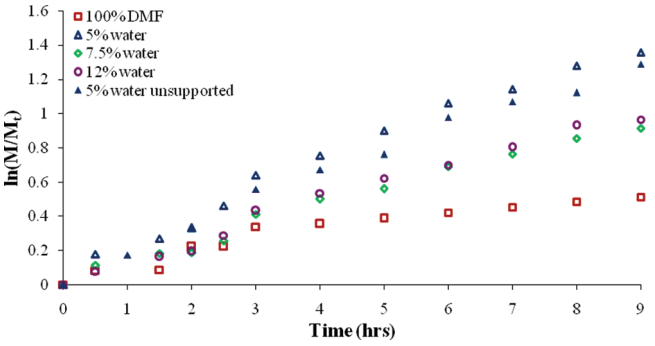


**Figure 3.** Kinetic plot showing rate of reaction against time in the L-proline catalyzed aldol reaction, at 20 mol % of copolymer **5c** with varying water concentrations and with unsupported L-proline at 5 vol % water for rate comparison; all conversions were determined by HPLC analysis.

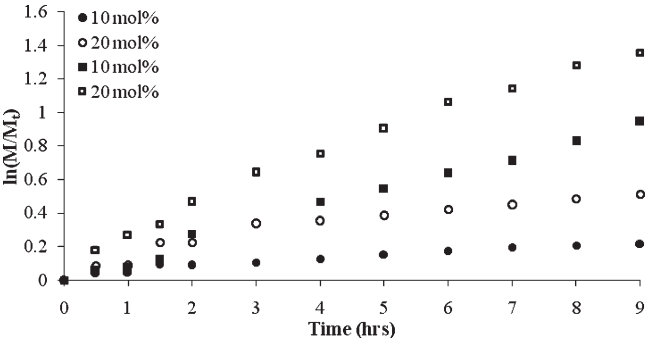


**Figure 4.** Kinetic plot comparing the rate of the aldol reaction in 100% DMF (○, ●) and in DMF/5 vol % water (□, ■), for polymer **5e** as determined by HPLC analysis.

successfully catalyzed the aldol reaction at 10 mol % catalyst loading and at relatively high comonomer incorporation.[59] To further explore the potential of the L-proline-supported system, the RAFT derived copolymers were synthesized with lower catalyst incorporation, ca. 5%. It was proposed that lowering the catalyst loading would change the copolymer's solution properties and aid in the recycling of the support. To confirm that the RAFT derived copolymer **5c** (as a representative example) was able to catalyze the aldol reaction with high yield and selectivity, the reaction was first carried out using 20 mol % catalyst loading. It was interesting to note that the reaction did indeed take place and that, with water as a cosolvent, reactions uniformly gave a higher conversion after 24 h compared to those reactions performed in the absence of water (Table 2).[60−62,76] The reaction with 5 vol % water present gave the best overall result (98% conversion, 95:5 anti:syn, 89% ee after 24 h), while those with supported L-proline at 7.5 and 12 vol % water gave lower conversions. The addition of more than 12 vol % water was not possible, as this caused the polymer-supported catalyst to precipitate out of solution, presumably due to the hydrophobic nature of the polystyrene.

To provide a direct comparison, the aldol reaction was carried out under the same conditions with unsupported L-proline at 20 mol % with 5, 7.5, and 12 vol % water (Table 2), all of which gave high conversion (98−99%) but slightly reduced enantioselectivity (82−88%) compared with the polymeric system (85−94%). Similarly to the supported system, when the unsupported L-proline reaction was carried out in pure DMF, a lower conversion after 24 h was observed, which was considerably lower than the polymer supported system. The kinetic plots for the unsupported L-proline catalyzed aldol reactions at different DMF/water ratios are shown in Figure S6.

A more detailed picture was obtained by monitoring the reaction progress at regular intervals over 9 h and then sampling after 24 h (Figure 3). The increased rate of reaction in the presence of water is clear from the data (after 9 h, 40% conversion in DMF vs 74% conversion with 5 vol % water in DMF); however, it appears that 7.5 vol % water or greater has a detrimental effect on the reaction rate of the supported L-proline (cf. after 9 h, ca. 60% conversion for 7.5 vol % water in DMF), likely due to the gradual reduction in polymer solubility at higher water contents. It is interesting to note that upon supporting L-proline onto a polymer scaffold its catalytic activity is retained, and importantly,

**Table 3. Comparison of the Activity and Selectivity of the Aldol Reaction Carried Out at 10 and 20 mol % Catalyst Loading after 24 h**

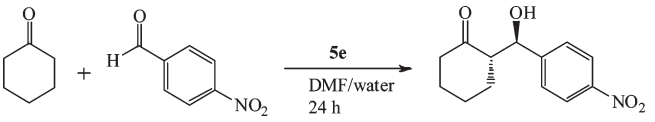


| entry | % water in DMF | mol % | % conv HPLC | % conv NMR | anti/syn[a] | % ee[b] |
|---|---|---|---|---|---|---|
| 1 | 0 | 20 | 50 | 49 | 89/11 | 91 |
| 2 | 5 | 20 | 90 | 98 | 95/5 | 89 |
| 3 | 0 | 10 | 27 | 38 | 85/15 | 87 |
| 4 | 5 | 10 | 95 | 95 | 95/5 | 93 |

[a] Determined by $^1$H NMR spectroscopy in $CDCl_3$. [b] Determined by chiral HPLC, ChiralPak IA column (80:20 hexane:IPA).

the supported system also shows high diastereoselectivity and enantioselectivity.

The aldol reaction was also carried out at 20 mol % catalyst loading with copolymer **5e** and **5b**, a higher and lower molecular weight polymer, respectively ($M_n$ = 11.6 and 5.0 kDa), in 100% DMF and 5 vol % water in DMF. The results obtained were comparable to those using **5c** and led to the conclusion that the rate and stereoselectivity of the reaction (e.g., for **5e** after 24 h, 96% conversion, anti/syn ratio 96/4, ee 98% (for **5c**, 98%, 88/12, and 85%) in the mixed solvent system) are comparable between polymer samples of differing molecular weight.

To further investigate the potential of our polymer-supported catalyst, using the most efficient conditions (5 vol % water in DMF), the aldol reaction was carried out at a lower catalyst loading (10 mol %). Figure 4 shows the differences in rate of reaction when the catalyst loading was reduced from 20 to 10 mol %. Regardless of catalyst loading, the reaction shows a distinct enhancement in rate in the presence of water; in 100% DMF, the rate for both catalyst loadings, throughout the 24 h is significantly reduced, generally reaching lower final conversions, anti/syn ratios, and enantiomeric excesses (ee) (Table 3, entries 1 and 3). However, in DMF with 5 vol % water, though the reaction proceeds more slowly for the first 9 h, final conversions, anti/syn ratios, and enantiomeric excesses after 24 h are not significantly different (Table 3, entries 2 and 4). Interestingly, the reaction using 20 mol % catalyst loading in 100%

**Table 4. Comparison of Noncatalyzed and Catalyzed Aldol Reaction under the Same Experimental Conditions**

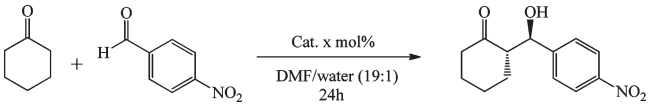


| entry | cat. | mol % | % conv[a] | anti/syn[b] | % ee[c] |
|---|---|---|---|---|---|
| 1 | no catalyst | — | | no reaction | |
| 2 | L-proline | 1 | 12 | 92/8 | 77 |
| 3 | L-proline | 5 | 57 | 90/10 | 94 |
| 4 | L-proline | 10 | 99 | 92/8 | 94 |
| 5 | L-proline | 20 | 99 | 90/10 | 97 |
| 6 | PS | — | | no reaction | |
| 7 | **5c** | 20 | 98 | 95/5 | 89 |
| 8 | **5e** | 1 | 57 | 95/5 | 91 |
| 9 | **5e** | 5 | 89 | 96/4 | 92 |
| 10 | **5e** | 10 | 95 | 95/5 | 93 |
| 11 | **5e** | 20 | 96 | 96/4 | 98 |

[a] Percentage conversion determined by $^1$H NMR spectroscopy in $CDCl_3$ after 24 h. [b] Determined by $^1$H NMR spectroscopy in $CDCl_3$ after work-up. [c] Determined by chiral HPLC, ChiralPak IA column (80:20 hexane:IPA).

DMF gives a similar outcome to that of 10 mol % catalyst loading in DMF with 5 vol % water, highlighting the importance of water for enhancing the performance of the catalyst and allowing for lower catalyst loadings.

To ensure the activity and selectivity observed are in fact related to the presence of our polymer-supported catalyst, additional reactions were carried out both with unsupported L-proline and with a nonfunctionalized polystyrene in the reaction mixture (in the absence of any catalyst). These reactions were carried out using the same conditions as previously discussed, in DMF with 5 vol % water for 24 h. The results are detailed in Table 4 and demonstrate the similarity in both activity and selectivity between our copolymer system and unsupported L-proline at comparable loadings. However, when lower loadings were used, i.e., 5 and 1 mol %, the difference in activity between supported and unsupported catalysts becomes greater. The performance of the unsupported L-proline is reduced to a greater extent than that of the supported system at lower loadings. At the lowest loading, 1%, unsupported L-proline reached 12% conversion in 24 h compared to 57% (with excellent anti/syn ratio and % ee) for the supported L-proline. These results further highlight the advantage of the polymer supported system.

**Characterization of Aldol Products.** $^1$H NMR spectroscopy was used to determine the diastereoselectivity of the reaction by comparing the signal for the proton labeled "d" at $\delta$ 4.82 (anti-H) and $\delta$ 5.41 (syn-H) in Figure S7. The selectivity of the polymer-supported catalyst, when carried out in the presence of water, is similar to that of unsupported L-proline, usually achieving diastereomeric ratios (dr) of at least 95/5 (see Table 2, entry 4). However, when carried out in 100% DMF, the L-proline/polystyrene system is superior to that of unsupported L-proline, achieving a selectivity of 75/25 or better, whereas the reaction does not proceed with unsupported L-proline, most likely due to lack of solubility (data not shown). This highlights how the presence of a polymer scaffold may widen the scope of solvents that can be used to catalyze reactions using organocatalysts such as L-proline. The enantioselectivity of the reaction was determined by HPLC, on a Chiralpak IA column, and the racemic aldol product was run as a point of reference. These results suggested the polymer-supported catalyst is capable of achieving high ee values, comparable to those obtained for unsupported L-proline. Generally, ee values of 90% or higher were found for the reactions catalyzed by copolymers **5**.

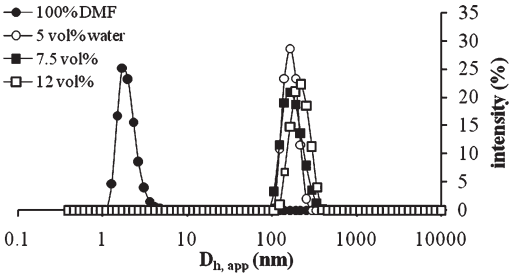


**Figure 5.** Graphical representation of DLS results, showing the size ($D_{h,app}$) of copolymer **5c** in different solvent systems (at 10 mg/mL).

**Self-Assembly of the Copolymer.** As previously mentioned, we hypothesized a gradient type profile of the two monomers in copolymers **5**. This profile is important as monomer **2** can be considered amphiphilic and hence may undergo a selective assembly process in mixed solvent systems to create a unique microenvironment for the L-proline catalyst, possibly influencing its catalytic behavior. Indeed, we wanted to further explore whether the observed increase in rate of the supported system in mixed solvent system was related to the formation of well-defined aggregates. The copolymers **5c** and **5e** were dissolved in DMF and in DMF with 5 vol % water and were examined by dynamic light scattering (DLS) and microscopy (TEM and SEM) techniques. Because of the high concentration of copolymer used in the aldol reactions (ca. 90 mg/mL), it was not possible to perform analysis via light scattering or light microscopy on the actual reacting systems; thus, a lower concentration (10 mg/mL) was used to characterize the copolymers solutions.

DLS studies of the fully dissolved copolymer **5c** in DMF gave hydrodynamic diameters of 3 nm (PD 0.204), indicating the presence of unimers in solution. However, upon the addition of water (at least 5 vol %) large structures with hydrodynamic diameters ($D_{h,app}$) of 160 nm (PD 0.171) were found, confirming a change from unimer polymer chains to chain association to form aggregates. A graphical representation of these results is shown in Figure 5. We also extended our analysis of copolymer **5c** by changing the DMF:water ratio to larger water contents. The difference in size between 5 and 7.5 vol % water (ca. 170 nm, PD ca. 0.25 in both cases) was not significant, and it was not until 12 vol % water had been added that a considerable increase in $D_{h,app}$ (220 nm, PD 0.327) was found. However, it should be noted that as the water content increased, a broadening in the polydispersity was found. The correlation functions of the DLS runs are shown in Figure S8. The size of the aggregates is larger than expected for conventional micelles, as they are over 100 nm and hence may be micelle aggregates, vesicles, or compound micelles.[77]

To further investigate the results obtained by DLS, the self-assembled structures were studied using TEM and SEM. For characterization by TEM, samples of copolymers **5c** and **5e** at 10 mg/mL were prepared. These were both deposited onto TEM grids that had previously been treated with oxygen plasma and subsequently stained with uranyl acetate (UA) or ammonium

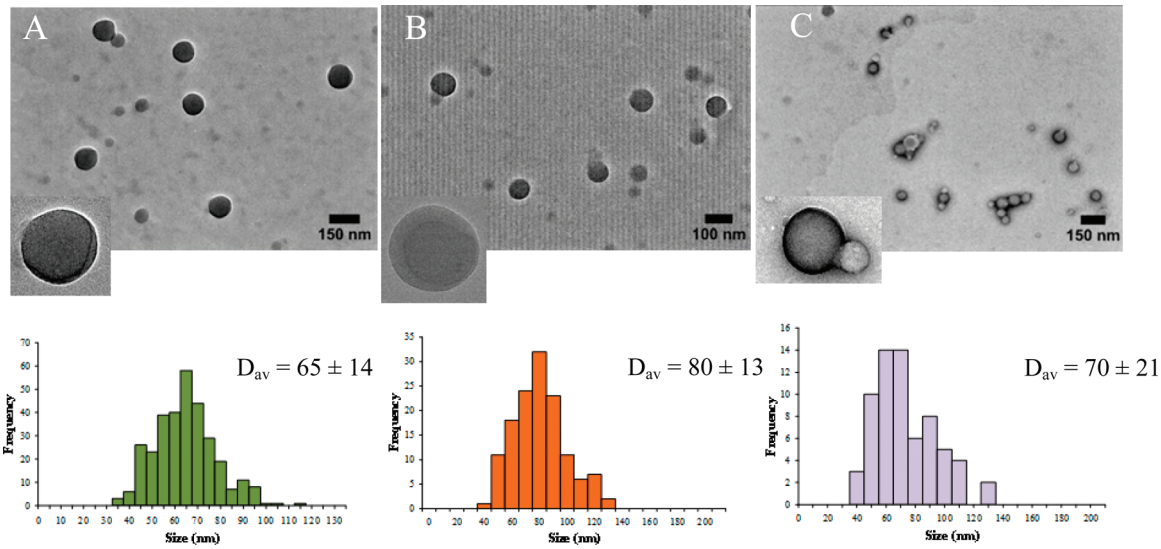


**Figure 6.** Representative TEM micrographs of **5c** in DMF with different vol % of water in DMF: (A) 5 vol %, (B) 7.5 vol %, and (C) 12 vol %, all stained with 2% AM with histograms showing the size distribution of **5c** ($D_{av}$ is in nm).

molybdate (AM) before imaging. Spherical structures were revealed in both stains, though large networks/clusters of aggregates were noted with UA, which were an artifact induced by staining (Figure S9) and individual structures with AM (Figure 6 and Figure S10). Thus, the sizes obtained from the two different stains cannot be directly compared. However, the size of the structures found does not seem to be concentration dependent, as similar sized structures were noted for both 10 and 2 mg/mL solutions. Figure 6 shows the TEM micrographs of **5c** in solutions at different water contents stained with AM, displaying small differences in particle size.

To confirm these observations, a second copolymer **5e** was additionally examined by DLS and TEM. Copolymer **5e**, differing only in molecular weight from **5c**, showed similar self-assembly behavior in 5 vol % water solutions. Histograms of the size distributions are also provided. Though DLS results for **5e** (210 nm, PD 0.247) differ from **5c** by 50 nm, the particle size obtained by TEM ($D_{av}$ = 90 ± 20 nm) does not differ significantly, confirming the formation of similar self-assembled aggregates. The difference in noted sizes is most likely due to copolymer **5e** having a longer polystyrene chain.

TEM analysis of these aggregates did not indicate a bilayer-type structure, and indeed minimal contrast variations inside particles were found suggesting a solid particle, despite the large size which is normally indicative of a vesicle-like or compound structure. To further explore the morphology of these particles, we imaged them using TEM on graphene oxide (GO) substrates. GO is an excellent support for the TEM analysis of low contrast samples as it is nearly electron transparent, and polymer nanostructures can be readily imaged without staining.[78] Particles formed from copolymer **5e** in 5 vol % water solutions were analyzed using GO as a support and solid although relatively disperse structures (ca. 75 nm) were confirmed. From Figure 7 we can clearly see that some particles are overlaid, and the resulting contrast could possibly indicate a flattened or disklike morphology. To explore this further, we performed some dry TEM tomography experiments (Figure S12). The 3D projection of the structures after reconstructing the tilt series (−45° to +45°) into a stack indicated structures are indeed spherical,

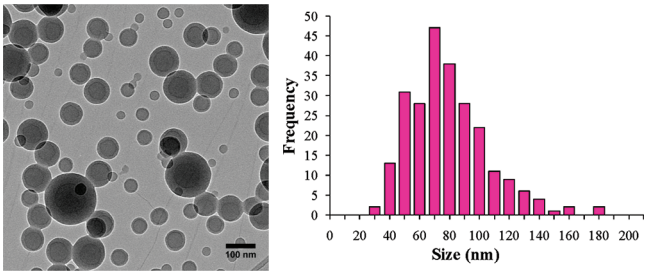


**Figure 7.** Representative TEM micrograph on GO of **5e** in DMF with 5 vol % water with histogram showing the size distribution of the aggregates.

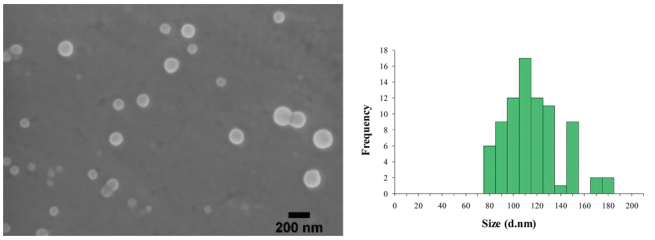


**Figure 8.** SEM micrographs of **5e** in a 5 vol % water solution, on an AM stained TEM grid, which was subsequently coated with gold with the histogram showing size distribution of **5e**.

and an orthogonal slice of the stack through the structures further confirmed that the particles are solid (Figure S13). We also were keen to explore these nanostructures in a hydrated state using cryo-TEM, and although the structures are much larger than observed by dry-state TEM, the spherical morphology was confirmed (Figure S14).

The aggregates found from copolymer **5e** were further characterized by SEM, and for direct comparison the stained grid used for TEM analysis was sputter-coated with gold and then studied by SEM. Indeed, the size obtained by SEM (110 ± 24 nm) was comparable to those previously obtained by TEM


dx.doi.org/10.1021/ma201256m |*Macromolecules* 2011, 44, 7233–7241

**Table 5. Recyclability of Polymer-Supported L-Proline, 5g, in the Aldol Reaction**

| cycle | 24 h conv[a] | anti/syn[a] | ee[b] | recovery (%) |
|---|---|---|---|---|
| 1 | 95 | 97/3 | 89 | 88 |
| 2 | 99 | 95/5 | 90 | 85 |
| 3 | 94 | 95/5 | 88 | 90 |

[a] Determined by $^1$H NMR spectroscopy, in $CDCl_3$. [b] Determined by chiral HPLC, ChiralPak 1A column (80:20 hexane:IPA).

(90 ± 20 nm). A representative SEM micrograph is shown in Figure 8, together with a histogram of the particle size distribution.

**Zeta Potential.** The zeta potential of the well-defined aggregates, specifically copolymer **5e**, was evaluated to explore the location of the L-proline functionalities, whether they are contained within the core or are present at the surface of the aggregates. The achieved zeta values at concentrations 2 mg/mL and 10 mg/mL were positive, 26.0 mV and 32.5 mV, respectively. These values suggest that the L-proline functionalities are not at the surface of the aggregates, as carboxylic acid groups on the surface of the aggregates would have resulted in negative zeta potentials. This finding supports our hypothesis that L-proline catalysis takes place within the contained microenvironment of the polymeric aggregates.

**Recycling.** The recycling potential of our polymer-supported catalytic system was studied using the previously discussed aldol reaction between 4-nitrobenzaldehyde and cyclohexanone, in the 5 vol % water/DMF solvent mixture. The copolymer **5g** (10.2 kDa, $D_{h,app}$ = 143 nm, PD = 0.202) employed for the recycling study was recovered from the reaction mixture via the dropwise addition of aqueous LiBr (50 mL, 4 wt %), which quenches the reaction and simultaneously, due to the insolubility of polystyrene in water, causes the copolymer to precipitate out of solution. Then, the precipitated polymer was filtered, washed with additional water, and dried in the vacuum oven at 40 °C. The aldol product was then extracted from the aqueous solution in the same manner as previously described. Once dried, the polymer was redissolved in DMF/5% water, and a second aldol cycle was carried out. The amount of reactants added to the new cycle was adjusted according to the amount of polymer recovered from the previous cycle. This adjustment was done to keep the aldol reaction at 10 mol % catalyst loading throughout the different cycles. Table 5 shows the recycling efficiency of our polymer-supported system. The catalyst was successfully used in 3 cycles without losing significant activity or selectivity, recovering ∼90% of the catalyst in each cycle. Attempts to recycle the lower molecular weight polymer, **5b**, led to less efficient recovery; hence, although the molecular weight does not affect the catalysis rate, it can influence the ease of recyclability.

## CONCLUSIONS

We report the use of RAFT copolymerization to controllably incorporate an amino acid (L-proline) containing monomer into a polystyrene backbone to yield copolymers with tunable catalyst loading. The organocatalytic activity and selectivity of these RAFT derived polymers were carefully studied in a model aldol reaction, resulting in conversions, diastereoselectivities, and enantioselectivities close to those achieved in unsupported L-proline catalysis but with higher activity and selectivity at low loadings when compared to unsupported L-proline. The major advantage of our polymer-supported catalyst system is the possibility of catalyst recovery and reuse in consecutive cycles without reducing the activity or selectivity of the catalyst. It was also evident that the functionalized copolymers self-assembled into well-defined aggregates in the DMF/water solvent system used to carry out the aldol reaction. We believe that the unique microenvironment for L-proline inside these self-assembled structures positively influences catalysis of the aldol reaction. Further work will explore the extension of these L-proline systems for applications in well-defined micellar catalysis.

## ASSOCIATED CONTENT

**Supporting Information.** Further characterization data for the monomer, CTA, and copolymers and copolymerization data along with characterization data for the nanostructures. This material is available free of charge via the Internet at http://pubs.acs.org.

## AUTHOR INFORMATION

**Corresponding Author**

*E-mail: dal28@cam.ac.uk (D.A.L.), r.k.o-reilly@warwick.ac.uk (R.K.O.).

## ACKNOWLEDGMENT

The EPSRC and Royal Society are thanked for financial support, as are the University of Cambridge and the University of Warwick through the research development fund. D.A.L. thanks Homerton College and the Department of Chemistry for support. T.P.S. and T.H.E. thank the NIH-NCRR COBRE (#P20RR017716) and NIST, U.S. Department of Commerce (#70NANB7H6178), for financial support. The statements herein do not reflect the views of NIH or NIST. The authors also acknowledge Courtney Ondeck and Dr. Amanda Evans for initial work in this area and Prof. van Herk (TU Eindhoven) for assistance and useful discussions with regard to reactivity ratios. Malvern instruments are acknowledged for assistance with zetasizer measurements. The GPC equipment used in this research was obtained through Birmingham Science City: Innovative Uses for Advanced Materials in the Modern World (West Midlands Centre for Advanced Materials Project 2), with support from Advantage West Midlands (AWM) and part funded by the European Regional Development Fund (ERDF). Finally, we acknowledge the University of Delaware Keck Microscopy Facility for use of their TEM and Vitrobot and the Center for Molecular and Engineering Thermodynamics for use of their DLS and SLS instruments.

## REFERENCES

(1) MacMillan, D. W. C. *Nature* **2008**, *455*, 304–308.
(2) Gaunt, M. J.; Johansson, C. C. C. *Chem. Rev.* **2007**, *107*, 5596–5605.
(3) Raj, M.; Singh, V. K. *Chem. Commun.* **2009**, 6687–6703.
(4) List, B.; Lerner, R. A.; Barbas, C. F. *J. Am. Chem. Soc.* **2000**, *122*, 2395–2396.
(5) Eder, U.; Sauer, G.; Wiechert, R. *Angew. Chem., Int. Ed.* **1971**, *10*, 496–497.
(6) List, B. *Tetrahedron* **2002**, *58*, 5573–5590.
(7) List, B.; Hoang, L.; Martin, H. J. *Proc. Natl. Acad. Sci. U. S. A.* **2004**, *101*, 5839–5842.
(8) Mukherjee, S.; Yang, J. W.; Hoffmann, S.; List, B. *Chem. Rev.* **2007**, *107*, 5471–5569.

(9) Movassaghi, M.; Jacobsen, E. N. *Science* **2002**, *298*, 1904–1905.
(10) Hajos, Z. G.; Parrish, D. R. *J. Org. Chem.* **1974**, *39*, 1615–1621.
(11) Notz, W.; Tanaka, F.; Watanabe, S.-i.; Chowdari, N. S.; Turner, J. M.; Thayumanavan, R.; Barbas, C. F. *J. Org. Chem.* **2003**, *68*, 9624–9634.
(12) List, B.; Pojarliev, P.; Castello, C. *Org. Lett.* **2001**, *3*, 573–575.
(13) Mase, N.; Thayumanavan, R.; Tanaka, F.; Barbas, C. F. *Org. Lett.* **2004**, *6*, 2527–2530.
(14) Bui, T.; Barbas, C. F. *Tetrahedron Lett.* **2000**, *41*, 6951–6954.
(15) Hoang, L.; Bahmanyar, S.; Houk, K. N.; List, B. *J. Am. Chem. Soc.* **2002**, *125*, 16–17.
(16) Notz, W.; Tanaka, F.; Barbas, C. F. *Acc. Chem. Res.* **2004**, *37*, 580–591.
(17) Mase, N.; Nakai, Y.; Ohara, N.; Yoda, H.; Takabe, K.; Tanaka, F.; Barbas, C. F. *J. Am. Chem. Soc.* **2006**, *128*, 734–735.
(18) Hayashi, Y.; Sumiya, T.; Takahashi, J.; Gotoh, H.; Urushima, T.; Shoji, M. *Angew. Chem., Int. Ed.* **2006**, *45*, 958–961.
(19) Cobb, A. J. A.; Shaw, D. M.; Longbottom, D. A.; Gold, J. B.; Ley, S. V. *Org. Biomol. Chem.* **2005**, *3*, 84–96.
(20) Veverková, E.; Strasserová, J.; Sebesta, R.; Toma, S. *Tetrahedron: Asymmetry* **2010**, *21*, 58–61.
(21) Bellis, E.; Kokotos, G. *Tetrahedron* **2005**, *61*, 8669–8676.
(22) Tang, Z.; Jiang, F.; Cui, X.; Gong, L.-Z.; Mi, A.-Q.; Jiang, Y.-Z.; Wu, Y.-D. *Proc. Natl. Acad. Sci. U. S. A.* **2004**, *101*, 5755–5760.
(23) Tang, Z.; Yang, Z.-H.; Chen, X.-H.; Cun, L.-F.; Mi, A.-Q.; Jiang, Y.-Z.; Gong, L.-Z. *J. Am. Chem. Soc.* **2005**, *127*, 9285–9289.
(24) Kristensen, T. E.; Hansen, T. *Eur. J. Org. Chem.* **2010**, 3179–3204.
(25) Benaglia, M.; Celentano, G.; Cozzi, F. *Adv. Synth. Catal.* **2001**, *343*, 171–173.
(26) Benaglia, M.; Cinquini, M.; Cozzi, F.; Puglisi, A.; Celentano, G. *Adv. Synth. Catal.* **2002**, *344*, 533–542.
(27) Benaglia, M.; Cinquini, M.; Cozzi, F.; Puglisi, A.; Celentano, G. *J. Mol. Catal. A: Chem.* **2003**, *204*, 157–163.
(28) Font, D.; Jimeno, C.; Pericas, M. A. *Org. Lett.* **2006**, *8*, 4653–4655.
(29) Gruttadauria, M.; Giacalone, F.; Marculescu, A. M.; Lo Meo, P.; Riela, S.; Noto, R. *Eur. J. Org. Chem.* **2007**, 4688–4698.
(30) Gruttadauria, M.; Salvo, A. M. P.; Giacalone, F.; Agrigento, P.; Noto, R. *Eur. J. Org. Chem.* **2009**, *2009*, 5437–5444.
(31) Liu, Y. X.; Sun, Y. N.; Tan, H. H.; Liu, W.; Tao, J. C. *Tetrahedron: Asymmetry* **2007**, *18*, 2649–2656.
(32) Font, D.; Bastero, A.; Sayalero, S.; Jimeno, C.; Pericas, M. A. *Org. Lett.* **2007**, *9*, 1943–1946.
(33) Miao, W. S.; Chan, T. H. *Adv. Synth. Catal.* **2006**, *348*, 1711–1718.
(34) Aprile, C.; Giacalone, F.; Gruttadauria, M.; Marculescu, A. M.; Noto, R.; Revell, J. D.; Wennemers, H. *Green Chem.* **2007**, *9*, 1328–1334.
(35) Bellis, E.; Kokotos, G. *J. Mol. Catal. A: Chem.* **2005**, *241*, 166–174.
(36) Sanda, F.; Endo, T. *Macromol. Chem. Phys.* **1999**, *200*, 2651–2661.
(37) Lokitz, B. S.; Stempka, J. E.; York, A. W.; Li, Y.; Goel, H. K.; Bishop, G. R.; McCormick, C. L. *Aust. J. Chem.* **2006**, *59*, 749–754.
(38) Skey, J.; Hansell, C. F.; O'Reilly, R. K. *Macromolecules* **2010**, *43*, 1309–1318.
(39) Skey, J.; O'Reilly, R. K. *J. Polym. Sci., Part A: Polym. Chem.* **2008**, *46*, 3690–3702.
(40) Casolaro, M.; Bottari, S.; Cappelli, A.; Mendichi, R.; Ito, Y. *Biomacromolecules* **2004**, *5*, 1325–1332.
(41) Kristensen, T. E.; Vestli, K.; Fredriksen, K. A.; Hansen, F. K.; Hansen, T. *Org. Lett.* **2009**, *11*, 2968–2971.
(42) Kristensen, T. E.; Vestli, K.; Jakobsen, M. G.; Hansen, F. K.; Hansen, T. *J. Org. Chem.* **2010**, *75*, 1620–1629.
(43) Monterio, M. *Macromolecules* **2010**, *43*, 1159–1168.
(44) Barner-Kowollik, C.; Perrier, S. *J. Polym. Sci., Part A: Polym. Chem.* **2008**, *46*, 5715–5723.
(45) Chiefari, J.; Chong, Y. K.; Ercole, F.; Krstina, J.; Jeffery, J.; Le, T. P. T.; Mayadunne, R. T. A.; Meijs, G. F.; Moad, C. L.; Moad, G.; Rizzardo, E.; Thang, S. H. *Macromolecules* **1998**, *31*, 5559–5562.
(46) Chong, Y. K.; Moad, G.; Rizzardo, E.; Thang, S. H. *Macromolecules* **2007**, *40*, 4446–4455.
(47) Goto, A.; Fukuda, T. *Prog. Polym. Sci.* **2004**, *29*, 329–385.
(48) Lowe, A. B.; McCormick, C. L. *Prog. Polym. Sci.* **2007**, *32*, 2 83–351.
(49) Moad, G.; Rizzardo, E.; Thang, S. H. *Aust. J. Chem.* **2005**, *58*, 379–410.
(50) Moad, G.; Rizzardo, E.; Thang, S. H. *Aust. J. Chem.* **2006**, *59*, 669–692.
(51) Moad, G.; Rizzardo, E.; Thang, S. H. *Polymer* **2008**, *49*, 1079–1131.
(52) Perrier, S.; Takolpuckdee, P. *J. Polym. Sci., Part A: Polym. Chem.* **2005**, *43*, 5347–5393.
(53) Willcock, H.; O'Reilly, R. K. *Polym. Chem.* **2010**, *1*, 149–157.
(54) Mori, H.; Iwaya, H.; Endo, T. *Macromol. Chem. Phys.* **2007**, *208*, 1908–1918.
(55) Mori, H.; Iwaya, H.; Nagai, A.; Endo, T. *Chem. Commun.* **2005**, 4872–4874.
(56) Mori, H.; Kato, I.; Matsuyama, M.; Endo, T. *Macromolecules* **2008**, *41*, 5604–5615.
(57) Mori, H.; Matsuyama, M.; Endo, T. *Macromol. Chem. Phys.* **2009**, *210*, 217–229.
(58) Evans, A. C.; Skey, J.; Wright, M.; Qu, W.; Ondeck, C.; Longbottom, D. A.; O'Reilly, R. K. *J. Polym. Sci., Part A: Polym. Chem.* **2009**, *47*, 6814–6826.
(59) Evans, A. C.; Lu, A.; Ondeck, C.; Longbottom, D. A.; O'Reilly, R. K. *Macromolecules* **2010**, *43*, 6374–6380.
(60) Blackmond, D.; Armstrong, A.; Coombe, V.; Wells, A. *Angew. Chem., Int. Ed.* **2007**, *46*, 3798–3800.
(61) Brogan, A. P.; Dickerson, T. J.; Janda, K. D. *Angew. Chem., Int. Ed.* **2006**, *45*, 8100–8102.
(62) Gruttadauria, M.; Giacalone, F.; Noto, R. *Adv. Synth. Catal.* **2009**, *351*, 33–57.
(63) Liu, Y.-X.; Sun, Y.-N.; Tan, H.-H.; Tao, J.-C. *Catal. Lett.* **2008**, *120*, 281–287.
(64) Zotova, N.; Franzke, A.; Armstrong, A.; Blackmond, D. G. *J. Am. Chem. Soc.* **2007**, *129*, 15100–15101.
(65) Dhaon, M. K.; Olsen, R. K.; Ramasamy, K. *J. Org. Chem.* **1982**, *47*, 1962–1965.
(66) Neises, B.; Steglich, W. *Angew. Chem., Int. Ed.* **1978**, *17*, 522–524.
(67) Ma, Q.; Wooley, K. L. *J. Polym. Sci., Part A: Polym. Chem.* **2000**, *38*, 4805–4820.
(68) Benaglia, M.; Chen, M.; Chong, Y. K.; Moad, G.; Rizzardo, E.; Thang, S. H. *Macromolecules* **2009**, *42*, 9384–9386.
(69) Benaglia, M.; Chiefari, J.; Chong, Y. K.; Moad, G.; Rizzardo, E.; Thang, S. H. *J. Am. Chem. Soc.* **2009**, *131*, 6914–6915.
(70) Skey, J.; O'Reilly, R. K. *Chem. Commun.* **2008**, 4183–4185.
(71) Fineman, M.; Ross, S. D. *J. Polym. Sci., Part A: Polym. Chem.* **1950**, *5*, 259–262.
(72) van Herk, A. M. *J. Chem. Educ.* **1995**, *72*, 138–140.
(73) Gallow, K. C.; Jhon, Y. K.; Tang, W.; Genzer, J.; Loo, Y.-L. *J. Polym. Sci., Part B: Polym. Phys.* **2011**, *49*, 629–637.
(74) Seno, K.-I.; Tsujimoto, I.; Kanaoka, S.; Aoshima, S. *J. Polym. Sci., Part A: Polym. Chem.* **2008**, *46*, 6444–6454.
(75) Font, D.; Sayalero, S.; Bastero, A.; Jimeno, C.; Pericas, M. A. *Org. Lett.* **2007**, *10*, 337–340.
(76) Zotova, N.; Franzke, A.; Armstrong, A.; Blackmond, D. G. *J. Am. Chem. Soc.* **2007**, *129*, 15100–15101.
(77) Zhang, L.; Eisenberg, A. *J. Am. Chem. Soc.* **1996**, *118*, 3168–3181.
(78) Williams, P. E.; Moughton, A. O.; Patterson, J. P.; Khodabakhsh, S.; O'Reilly, R. K. *Polym. Chem.* **2011**, *2*, 720–729.